Near-Bottom Currents off Southern California

The discharge of suspended wastewater solids from an ocean outfall may change the composition of the sediments and alter the community structure of biota living on and in the sediments (Greene and Sarason 1974, Greene and Smith 1975). These effects are influenced by the chemical composition of the particulates, the flux of particle mass to the bottom, resuspension and dispersion of deposited particles, and accumulation of particle mass in the sediments.

Studies on the mainland shelf off Southern California with sediment traps and transmissometers suggest that low level (chronic) resuspension may be common and potentially important in determining the fates of effluent particles. The bulk of resuspended sediments may be confined to within 5 m of the bottom (SCCWRP 1986, Hendricks 1987). Therefore, near-bottom currents will govern the dispersion and accumulation of resuspended particles. Measurements made by SCCWRP off Encinitas and by Karl *et al.* (1980) on the San Pedro Shelf suggest that the properties of near-bottom flows differ from the properties of mid water currents.

Retrieving the anchor for a mooring.

Since the late 1970s, SCCWRP has measured currents 1-3 m above the bottom from San Diego to Oxnard. Measurements were made primarily on the mainland shelf in water depths between 17 and 100 m; most of the measurements were made between 35 and 65 m. Near-bottom measurements were made at 150 m and 350 m on the upper slope off Newport Beach. Some of these measurements were used in models simulating the fates of particulates discharged from ocean outfalls (Hendricks 1983, Hendricks and Eganhouse 1992).

The objective of this study was to describe the properties of near-bottom currents on the mainland shelf and upper slope, and to compare them to mid water currents.

Materials and Methods

Measurement Locations

Near-bottom current measurements were made between 1979 and 1993 (Table 1). The most intensely sampled area was off Newport Beach near the County Sanitation Districts of Orange County municipal wastewater outfall.

Current Meters

Except for one deployment in 1993 with an InterOcean S4 current meter, all measurements in this report were made with negatively buoyant, aluminum inclinometer current meters (see *SCCWRP*

Table 1.

Summary of near-bottom current measurements made by SCCWRP between 1979 and 1990.

LOCATION	WATER DEPTH (M)	METER-MONTHS	NO. MOOR/DEPLOY
Point Loma (San Diego)	30, 35, 55, 77, 100	14	1-4
Encina (Carlsbad)	25, 45	17	2-3
Oceanside	40	2	1
Orange County-shelf	~56	23	1-2
Orange County-upper slope	150, 350	10	1
White Point (Palos Verdes)	25, 32, 60	7	1
Santa Monica Bay	36, 57, 73, 98	19	1-4
Oxnard	17	1	1

Inclinometer Current Meters in this volume).

Until 1989, the SCCWRP meters recorded only current speed and direction. Internal temperature measurements (0.1°C) were added to the speed and direction time series in 1986. Prior to 1992, data were recorded on film; after that time, measurements were made with a microprocessor-controlled current meter and the data, including temperature (0.05°C), were stored in solid state memory. The extensive set of records from the mainland shelf and upper slope off Newport Beach, and the more detailed information available with the electronic meters, biases the observations toward this area.

Near surface (11-15 m depth) measurements off Newport Beach were made with an InterOcean S4 electromagnetic current meter between 1989 and 1992. Data were collected for one month (10/93) with this meter 1.8 m above the bottom (mab). Burst sampling mode was used in all deployments of the S4. Velocity, temperature, and depth values were collected at 0.5 s intervals, combined, and averaged over a 2 s period. The 2 s average values were collected and recorded for either 9 min or 17 min to generate one set of "burst" samples. The bursts were repeated at 1.5 h intervals (burst duration 9 min) or 3 h intervals (burst duration of 17 min). The average of the 2 s observations within a burst was the average value of velocity, temperature, and pressure for the burst interval.

Subsurface taut line moorings were used in all deployments. The inclinometer current meters were suspended 1-3 mab. The original moorings used a bottom tag line connected to a separate surface mooring. Beginning in mid-1982, we used a taut line mooring with an acoustic release. At roughly monthly intervals, the moorings were recovered, the data retrieved, the meters and mooring serviced, and redeployed.

Data Processing

Observations in the film version of the current meter were recorded at 15 min intervals. However, sampling intervals of 45 min produced transport estimates that were not significantly different from sampling intervals of 15 min. The sampling interval was increased to 45 min to reduce the labor required to transcribe the data from the film. Data were collected and analyzed at 5 min intervals with the microprocessor-based version.

Current meter tilt was converted into current speed based on a tow-tank calibration for each meter. The time series of current speed and direction was used to generate a time series of “longshore” and “cross-shore” current velocities. The directions were aligned with the major principal and minor principal axes of variation of the slowly varying fluctuations (subtidal frequency band) in the mid water currents. The major principal axis was usually aligned with the isobaths (contours of constant water depth) at the mooring.

To determine this alignment, a trial velocity time series was constructed for each speed/direction file. The alignment of the trial “x-axis” was roughly parallel to the local isobaths. A 24.75 h running average filter applied to this time series produced a “low-pass” time series. A corresponding "high-pass" time series was constructed by subtracting the low-pass time series from the original velocity time series. The high-pass time series was dominated by fluctuations of tidal or higher frequency; the low-pass time series was dominated by subtidal fluctuations and net flow. The principal major axis for variations in the low-pass time series was computed to determine the alignment of the “longshore” axis. Next a new velocity time series was constructed from the speed/direction time series using this alignment. The x-axis was aligned so that positive velocities represented upcoast flow. The cross-shore axis was rotated 90° clockwise from the principal major axis, so positive values represented onshore flows. New low-pass and high-pass time series were constructed as before.

Kinetic energy (variance) of currents is distributed among a range of time scales. Partitioning was estimated by transforming the observed time series of velocities (i.e., in time space) into an orthogonal set of sine functions that form a basis set in frequency space (Ontnes and Enochson 1978). The range of frequencies for the sine functions spans from one-half the sampling frequency to one cycle during the deployment period. The amplitude of each frequency is its variance contribution to the total variance in the time series (Press *et al.* 1993). The transformation from time-space to frequency-space was done with a base-two discrete fast fourier transform (FFT). The net flow was returned as the amplitude at “zero” frequency. The time series was not detrended prior to the transformation. Time series with observations within 10% of a higher power of two were “padded” with zeros to increase the number of observations (Press *et al.* 1993), otherwise the number of observations was truncated to the largest power of two in the time series.

The contributions of the various frequencies to the total variance were examined in terms of a frequency- (or periodicity-) dependent cumulative variance. The square of the amplitude of each term is the variance contributed by each frequency (or periodicity) band in the series. The individual variances associated with periodicities shorter than a reference period were summed to obtain the total variance contributed by all variations shorter than the reference periodicity (or higher frequency).

Correlations between pairs of time series were computed by multiplying term by term the deviations from the average velocities without leading or lagging. The cross-products were summed and normalized to a maximum of unity by dividing by the product of the root-mean-square (rms) deviations for the two time series.

The cross-shore flux of temperature (surrogate for density) associated with fluctuations in water temperature and the cross-shore component of currents was also computed. Correlations between these variables can produce an onshore or offshore flux (e.g., Reynolds flux) even though there was no change in the average values of the variables. Low-pass and high-pass temperature time series were produced with a 24.75 h running average filter. The high-pass temperature time series, and corresponding high-pass cross-shore velocity time series, were multiplied term by term to produce a time series of cross-shore temperature fluxes. The temperature flux time series was filtered with a 24.75 h running average to generate a low frequency (subtidal band) time series representing changes in the daily-average Reynolds temperature fluxes. Correlations between the daily average cross-shore flows and the daily-average Reynolds flux of temperature were examined by multiplying and summing the terms of the low-pass velocity and Reynolds temperature flux time series. The deployment-averaged Reynolds temperature flux associated with slowly varying changes (subtidal frequency band) was computed from the product of the low-pass temperature time series and the low-pass cross-shore velocity time series.

Results

Temporal Variation in Currents

Currents on the mainland shelf off Southern California varied over time scales ranging from seconds to years and the temporal characteristics of longshore flows differed from the temporal characteristics of cross-shore flows. Fluctuations in the longshore component occurred at about two cycles per day (semi-diurnal tidal period) (Figure 1). Substantial changes also occurred over times ranging from days to the deployment period. The amplitudes of slowly changing fluctuations (subtidal frequency band) were suppressed in the near-bottom flows relative to the mid water flows. Fluctuations of tidal period were often enhanced in the near-bottom flows (not evident in Figure 1).

One of the most important differences between the cross-shore and longshore flows was a reduction in the amplitude of slowly varying changes at all depths in the cross-shore direction (Figure 2). Cross-shore motions were suppressed by the coastal barrier and the geostrophic character of flow. The amplitudes of semidiurnal fluctuations were enhanced in near-bottom cross-shore flows relative to mid water semi-diurnal tidal fluctuations. Fluctuations shorter than the tidal periods (supertidal frequency band) also made a greater contribution to the total variability of near-bottom flows compared to mid water flows.

The temporal distribution of cumulative variance for longshore flows increased at a relatively constant rate to an abrupt increase at 0.5 days (Figure 3), which corresponds to the energy (variance) associated with the semidiurnal tidal period. The increase in variance in near-bottom flow was substantially greater than the increases in variance in mid water flows. Fluctuations with periods close to one day (circa the diurnal tidal period and an inertial period of 22 h) were significant only at the shallowest depth (11 m). The relative contributions of variations at semidiurnal and diurnal tidal frequencies varied from deployment to deployment. In some deployments, there was a small contribution to the total variance by fluctuations with a period of about 0.25 days (first harmonic of the semi-diurnal tidal frequency) at the upper and lower current meters.

A steep increase in the variance of mid water longshore flows occurred at periods greater than one week (Figure 3). This corresponded to slowly varying changes in currents (Figure 1) and contributed more than half of the total variance in the longshore component of flow. In the near-bottom flow however, frequency fluctuations in longshore motions at subtidal periods were essentially absent. The total variance for near-bottom currents was substantially less than for mid water currents — even though tidal contributions to the variance were often greater near the bottom.

The temporal properties of variance for the cross-shore component of the flows differed from the longshore component. Contributions in the subtidal frequency band were greatly reduced in mid water and near-bottom flows, but increased with elevation above the bottom (Figure 4). This trend was consistent

Figure 1.

Longshore time series of currents off Newport Beach in 55 m of water from 1/24/92 to 2/25/92. The data (from bottom to top) are from elevations of 1, 3, 10, and 32 m above bottom (depths of 54, 52, 45, and 23 m below the surface). Positive values are upcoast flows (towards 270° magnetic); negative values are downcoast flows.

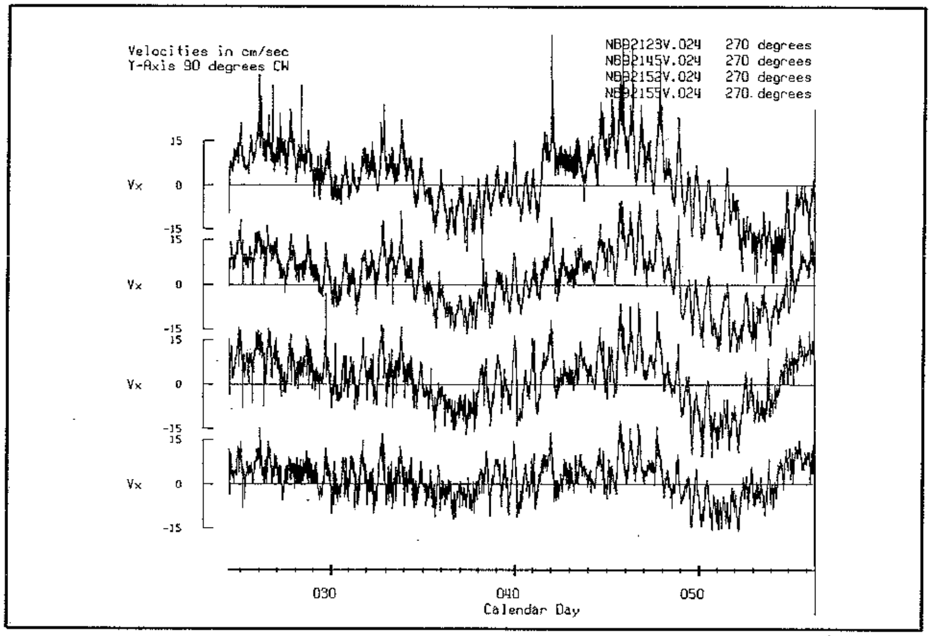

Figure 2.

Longshore time series of currents off Newport Beach in 55 m of water 1/24/92 to 2/25/92. The data (from bottom to top) are from elevations of 1, 3, 10, and 32 m above bottom (depths of 54, 52, 45, and 23 m below the surface). Positive values are onshore flows; negative values are offshore flows.

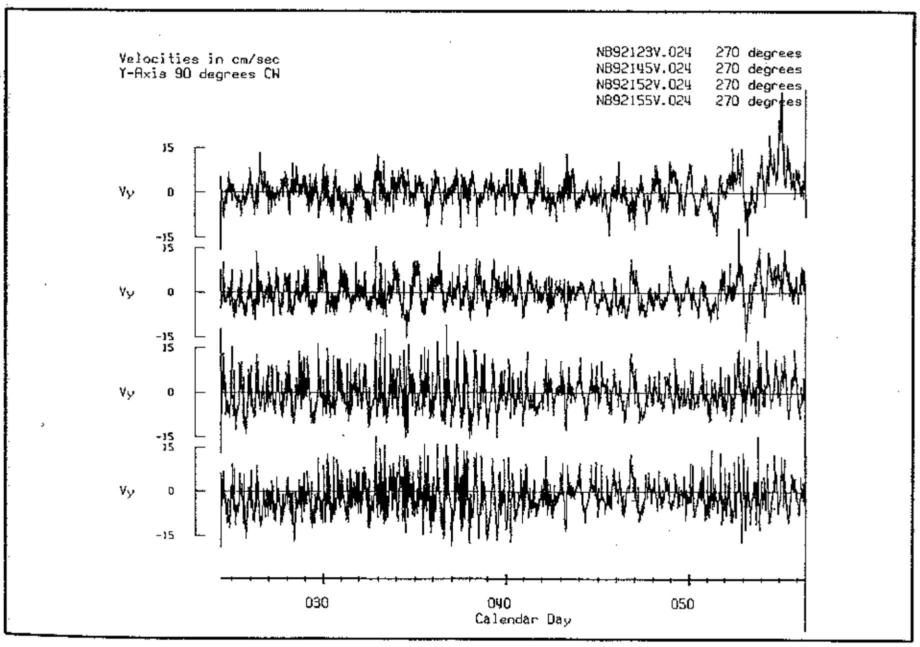

with an increasing separation between the current meters at each depth and the distance to its effective coastal boundary (isobath equal to meter depth). Short period fluctuations in the supertidal frequency band accounted for about half of the total variance in near-bottom flows. Semidiurnal fluctuations were greatest near the bottom, and minimal in mid water. Fluctuations of the first harmonic of semidiurnal tidal frequency did not contribute significantly to the total variance in the cross-shore component of the currents.

During the deployment off Newport Beach, the total cross-shore variance associated with tidal and supertidal frequency bands was less than for the longshore variations in the same frequency bands (Figure 4). At other times, depths, and locations, this relation was reversed — the cross-shore variance in these bands exceeded the longshore variance.

Current Speeds

Bottom friction reduced the speed of slowly varying fluctuations in near-bottom currents relative to mid water flows (Figure 5). Median speeds were about 11 cm/s 11 m below the surface, 9 cm/s at 36 m, and 6.5 cm/s at 54 m. About 10% of mid water observations had speeds greater than 23 cm/s and 10% of near-bottom flows had speeds greater than 14.5 cm/s.

The distribution of current speeds varied with location, depth, season, and year (Table 2). In Santa Monica Bay, the change between summer and winter was about 50%; off Palos Verdes, the seasonal change was about 20%. The largest seasonal change occurred off Carlsbad in 1986; the median speed of near-bottom currents was 6.5 cm/s in 45 m of water, and the 10-percentile speed was 13.5 cm/s. During summer, the median near-bottom speed fell to 3.5 cm/s and the 10-percentile speed declined to 6 cm/s. Near-bottom currents in 25 m of water were about twice as strong as near-bottom currents in 45 m of water. Off Point Loma, the median near-bottom speed increased from 7.3 cm/s in 35 m of water to 12.0 cm/s in 100 m of water.

Net Currents

There was a seasonal pattern in net longshore flows at all depths off Newport Beach — downcoast from early December to early May and upcoast the rest of the year (Figure 6). Net longshore velocities in 55 m of water averaged over the year were -0.6 cm/s at 11 m, 4.4 cm/s at 36 m, and 1.5 cm/s at 54 m. The difference between net flows at 11 m and 36 m was due to density stratification of the water column. The current meter at 11 m was in the

Figure 3.

Cumulative variance of the longshore component of coastal currents off Newport Beach in 55 m of water from 9/27/90 to 10/28/90. Vertical axis is the total variance associated with all fluctuations with periodicities shorter than the reference period (horizontal axis).

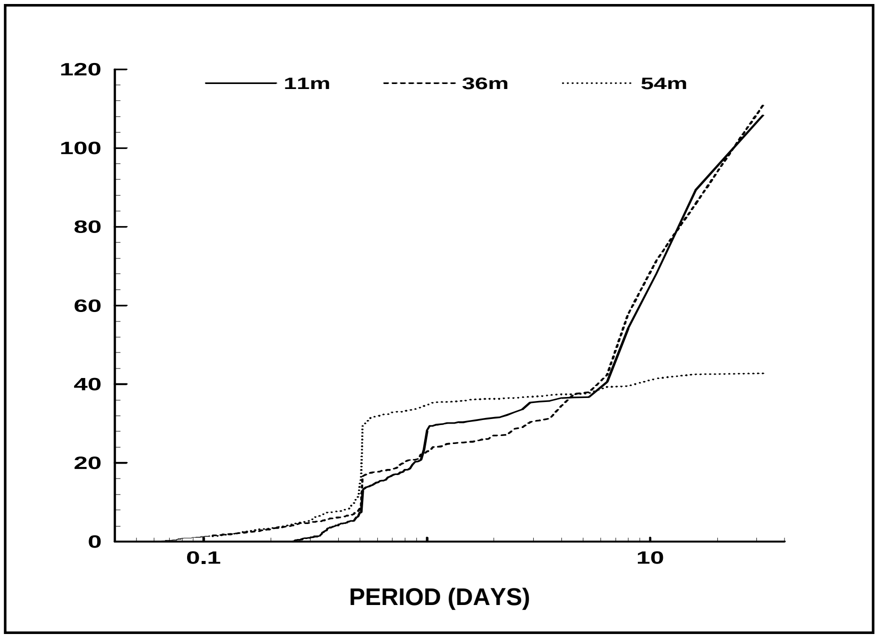

Figure 4.

Cumulative variance of the cross-shore component of coastal currents off Newport Beach in 55 m of water from 9/27/90 to 10/28/90. Vertical axis is the total variance associated with all fluctuations with periods shorter than the reference period (horizontal axis).

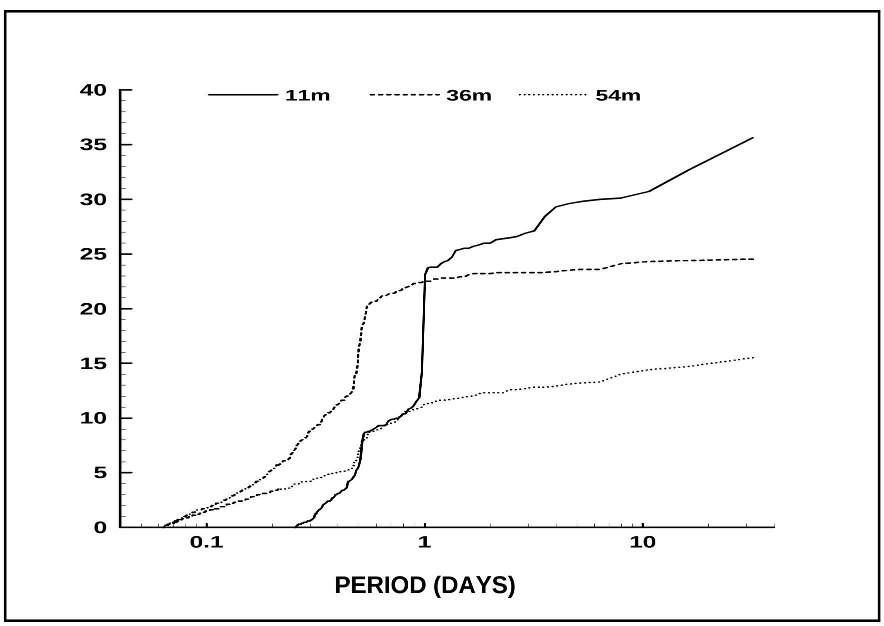

Table 2.
Summary of mid water and near bottom current speeds on the mainland shelf in the Southern California Bight between 1979 and 1993. D=depth; ratio=ration of bottom speed to midwater speed.

		CURRENT SPEED (CM/S)					
	DEPTH	MEDIAN (50%)			10% HIGHEST		
LOCATION	(m)	Mid	Bottom	Ratio	Mid	Bottom	Ratio
Pt. Loma (winter)	35	-	7.3	-	-	12.4	-
Pt. Loma (winter)	67	11.7	8.3	0.71	21.6	18.0	0.83
Pt. Loma (winter)	77	12.4	12.3	0.99	21.1	21.7	1.03
Pt. Loma (winter)	100	13.7	12.0	0.88	24.6	20.7	0.84
Carlsbad (winter)	45	8.6	6.5	0.76	15.0	8.7-13.1	0.73
Carlsbad (summer)	45	7.0-9.5	3.7-5.4	0.55	12.8-15.4	6.3-10.2	0.59
Oceanside (summer)	45	7.6	6.0	0.79	13.0	10.4	0.80
Newport Beach (all)	56	9.0	6.5	0.72	23.0	14.5	0.63
Palos Verdes (winter)	32	7.6	5.9	0.78	16.7	11.0	0.66
Palos Verdes (sprng)	60	6.7	7.2	1.07	16.1	13.1	0.81
SM Bay (summer)	55	9.9	8.1	0.81	15.8	16.6	1.05
SM Bay (winter)	55	10.8	12.3	1.14	20.5	21.7	1.06
SM Bay (spring)	55	8.3	8.6	1.03	16.6	17.2	1.04
Oxnard (fall)	17	11.3	7.7	0.68	21.1	14.0	0.66
Average	-	9.4	7.4	0.79	18.3	13.9	0.76

transition region between a net downcoast, surface mixed layer flow and a net upcoast flow below the thermocline. Reductions in net speed of near-bottom flows were due to friction with the bottom.

There was no seasonal pattern in net near-bottom cross-shore flows off Newport Beach (Figure 7). There was a persistent offshore flow that ranged from 1.6 to 3.6 cm/s (mean=2.3 cm/s). Net cross-shore flows in mid water varied from onshore in January through May to offshore in June through December. The annual net velocity was 0.2 cm/s offshore at 36 m and 0.4 cm/s onshore at 11 m. The lack of strong net cross-shore flows at mid water depths, but a persistent net offshore flow (comparable in magnitude to the net longside flow) near the bottom, was typical of current measurements on the mainland shelf.

Net mid water flows on the mainland shelf were approximately parallel to the longshore axis (i.e., principal major axis for fluctuations in the subtidal frequency band) (Table 3). A net offshore mid water flow was present in 35% of the 126 monthly data sets, but the seasonally-averaged mid water flow was about 0.3 cm/s onshore. In contrast, near-bottom net flows usually had a net offshore component; only 2.5% of the 78 near-bottom data sets had a net onshore flow (winter deployments off Palos Verdes). The seasonally averaged net flow near the bottom for all sites was 1.7 cm/s offshore.

On the mainland shelf, net cross-shore near-bottom velocities (1.1 cm/s offshore) were only slightly weaker than the net longshore near-bottom

Figure 5.

Distribution of current speeds in 55 m of water off Newport Beach from 10/26/89 to 10/31/90 plotted on a probability scale. The vertical axis is the percent of measurements with a speed below a reference speed (horizontal axis). A normal distribution of current speeds would plot as a straight line.

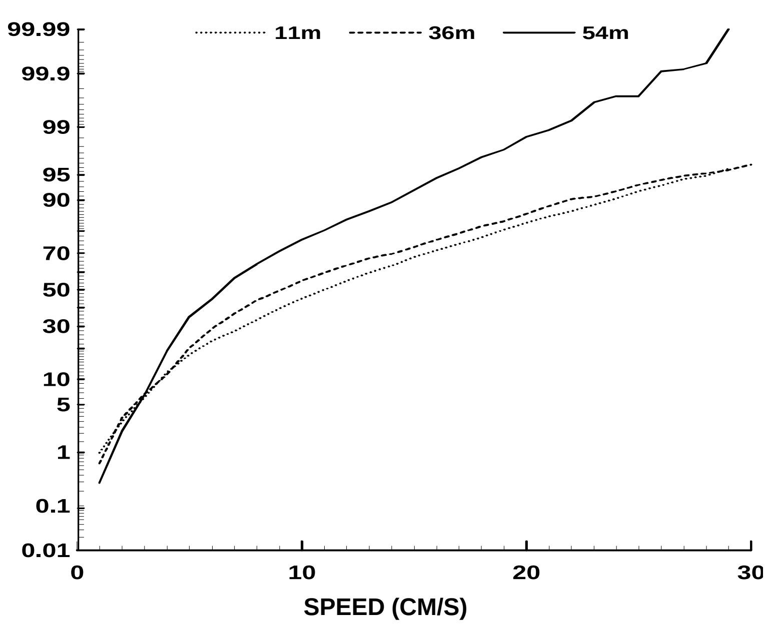

Figure 6.

Net longshore current speeds averaged over 12 deployments (about 1 month) in 55 m of water off Newport Beach from 10/26/89 to 10/31/90. The horizontal axis is the first day for each deployment period. Positive values are upcoast flows; negative values are downcoast flows.

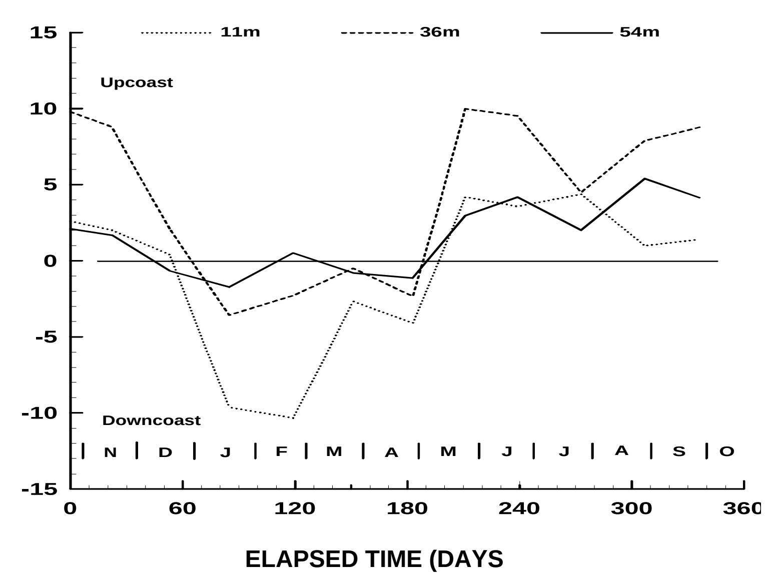

velocities (1.6 cm/s upcoast) (Figure 8). Eighty percent of the cross-shore velocities fell between 0.3 and 3.0 cm/s offshore, while 80% of the longshore velocities fell between 0.8 cm/s downcoast and 3.7 cm/s upcoast. Only 8% of the near-bottom net cross-shore flows were onshore and 18% of the near-bottom net longshore flows were downcoast. The strongest net cross-shore velocity was 5.2 cm/s offshore and the strongest net longshore velocity was 5.5 cm/s upcoast.

Near-bottom Currents on the Upper Slope

On the upper slope off Newport Beach, the seasonally-averaged mid water (50 and 100 mab) net cross-shore flows in 350 m of water were 0.1 cm/s (±0.3 cm/s) onshore. The seasonally averaged net near-bottom (1-2 mab) flows were 0.3 cm/s (±0.1 cm/s) onshore for eight months. Net near-bottom flows farther up the slope in 150 m of water had a seasonally averaged speed of 0.1 cm/s (±1.0 cm/s) onshore for one month in summer and one month in winter. There was no evidence for a net offshore or onshore near-bottom flow on the upper slope.

Thickness of the Layer of Net Offshore Flow on the Shelf

Net offshore transport near the bottom off Newport Beach was limited to about the lower

Figure 7.

Net cross-shore current speeds averaged over 12 deployments (about one month) in 55 m of water off Newport Beach from 10/26/89 to 10/31/90. The horizontal axis is the first day for each deployment period. Positive values onshore flows; negative values are offshore flows.

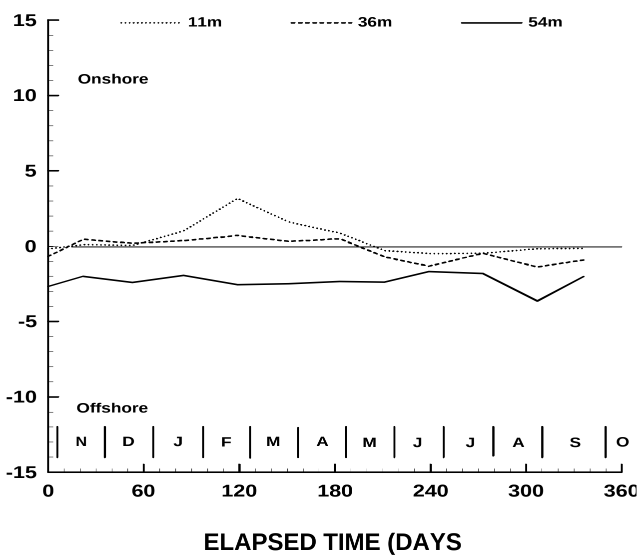

5 m of the water column (Figure 9). The net flow was uncertain above 5 m, although there was a weak net onshore flow at 10-20 mab.

Spatial Correlations Between Currents

Correlations (r) were calculated between near-bottom and mid water flows in the subtidal band measured at the same mooring (vertical separation), and between bottom flows at two moorings (horizontal separation) on the 56 m isobath off Newport Beach. The primary mooring had an InterOcean S4 current meter at 15 m, and inclinometer current meters at depths of 23, 45, 52, and 55 m (elevations of 41, 33, 11, 4, and 1 mab). The secondary mooring

Table 3.

Summary of net near-bottom current speeds on the mainland shelf in the Southern California Bight between 1979 and 1993. V=velocity in cm/s; N=number of deployments (about 1 month).

	WINTER		SPRING		SUMMER		WINTER	
LOCATION/DEPTH	Vy	N	Vy	N	Vy	N	Vy	N
Midwater								
Point Loma	1.6	11	-	0	0.2	8	-2.1	4
Carlsbad	0.5	5	1.6	3	0.5	8	-	0
Newport Beach	-0.2	3	0.2	11	-1.1	8	-0.3	13
Palos Verdes	0.7	8	0.5	9	0.2	1	1.2	4
Santa Monica Bay	0.2	7	0.9	8	0.4	7	0.7	7
Average/total	*0.8*	*34*	*0.6*	*31*	*0.0*	*32*	*-0.1*	*28*
Near bottom								
Point Loma	-3.1	6	-	0	-1.0	6	-4.9	2
Carlsbad	-1.6	8	-	0	-1.8	5	-2.1	4
Newport Beach	-2.2	4	-1.5	5	-1.7	6	-2.0	7
Palos Verdes	0.8	2	-0.4	5	-	0	-	0
Santa Monica Bay	-2.4	2	-1.4	5	-1.7	6	-2.4	6
Average/total	*-2.0*	*22*	*-1.1*	*15*	*-1.5*	*23*	*-2.5*	*19*

Figure 8.

Distribution of net near-bottom longshore and cross-shore current speeds from 83 (about 1 month) deployment-averaged velocities from Point Loma, Carlsbad (Encina), Newport Beach, Palos Verdes, Santa Monica Bay. A normal distribution of velocities would plot as a straight line.

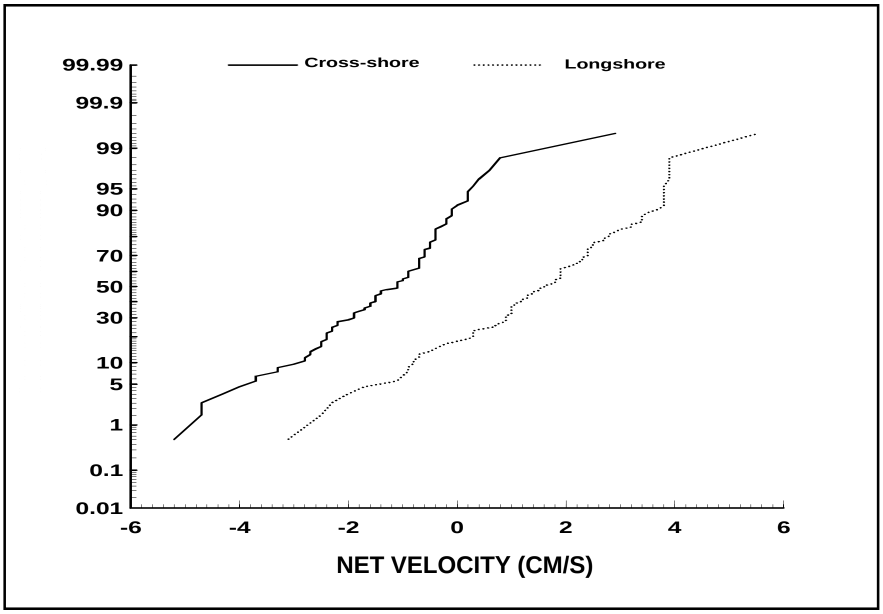

Figure 9.

Average net cross-shore current velocity near the bottom for five month long deployments off Newport Beach between 1989 and 1993. Light dashed lines are least-squares best linear fits for data between 0-5 m and 4-20 m above bottom. 19NN.nnn is the year (19NN) and the first calendar day (nnn) of deployment.

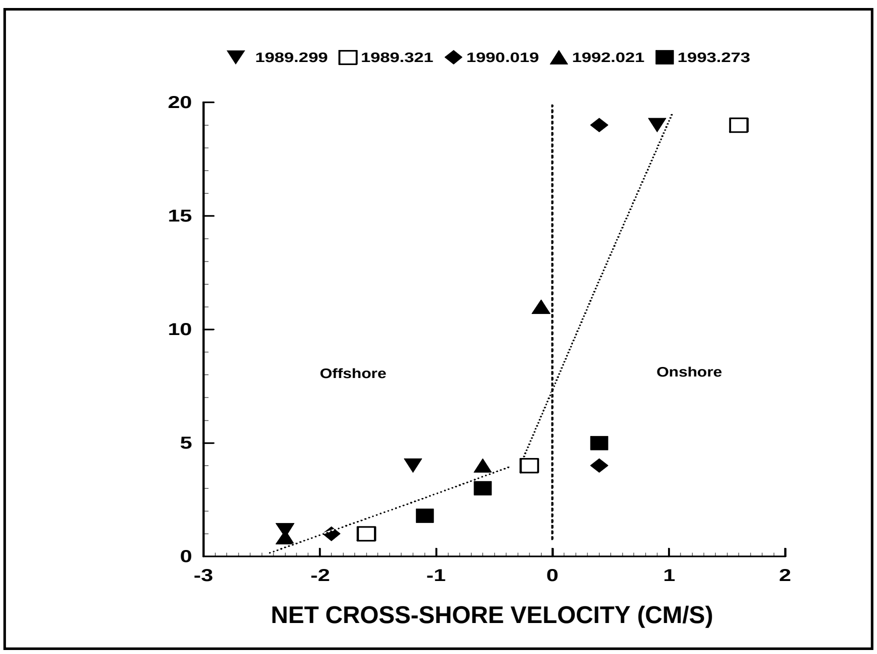

had inclinometer current meters at depths of 23, 34, 45, 52, and 55 m (elevations of 33, 22, 11, and 1 mab). The secondary mooring was 3.1 km upcoast from the primary mooring.

Vertical Separation

Correlations in the subtidal frequency band between current velocities near the bottom and velocities in mid water decreased with height above the bottom (Figure 10). For the longshore component of velocity, the correlation decreased at about 0.009/m between the bottom and a depth of 23 m. The correlation between the shallowest current meter (15 m depth) on the primary mooring and the near-bottom meter (55 m depth) was 0.63.

The rate of change in the correlation between mid water and near-bottom cross-shore flows in the subtidal frequency band differed between moorings. At the downcoast (primary) mooring, cross-shore flows in the subtidal frequency band were uncoupled from the near-bottom currents within 10 m of the bottom. The correlation between the current 1 mab and the current 11 mab was 0.05. At the upcoast (secondary) mooring, the correlation between the current 1 mab and the current 23 mab was 0.52; the correlation between the current 1 mab and the current 34 mab was 0.66.

Horizontal Separation

Correlations were 0.87-0.96 between longshore motions in the subtidal frequency band at current meters paired by depth on two moorings 3 km apart (Figure 11). The correlations for longshore fluctuations in tidal and supertidal frequency bands were lower. At elevations greater than 5-10 mab, correlations in the tidal band (0.62-0.67) were nearly independent of depth, but near the bottom, correlations declined to 0.48.

Correlations were 0.62-0.70 for cross-shore fluctuations in the subtidal frequency band. The trends were similar to those for longshore fluctuations, but the magnitudes were about 0.25 smaller. In the tidal and supertidal frequency band, the correlation declined sharply in the lower 5-10 m of water. The correlation also declined to 0.32 between the 44 m and 24 m depths.

Discussion

Net Offshore Flows

The properties of near-bottom currents on the mainland shelf off Southern California differed from the properties of currents higher in the water column. One of the most important differences was the presence of a net offshore component to cur-

Figure 10.

Correlations (r) between near-bottom and mid water currents measured by meters on the same mooring. There were two moorings in 56 m of water off Newport Beach from 1/25/92 to 2/25/92; mooring 2 was 3.1 km upcoast from mooring 1. Circles and squares are correlations between the bottom current meter and the meters above it on both moorings.

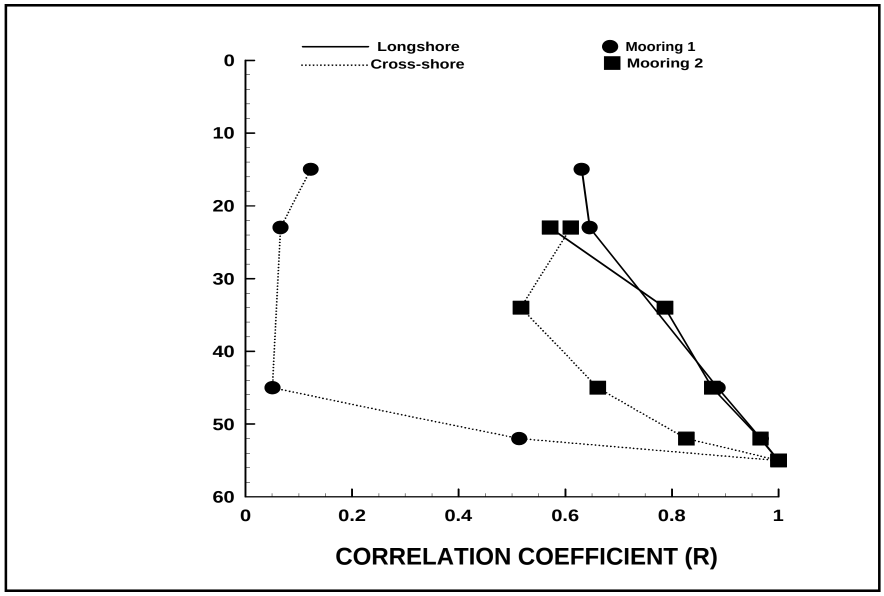

Figure 11.

Correlations (r) of longshore and the cross-shore flows between two moorings in 56 m of water off Newport Beach from 1/25/92 to 2/25/92. Meters were at the same depth on moorings separated by 3.1 km. Circles are correlations for fluctuations in the subtidal frequency band; squares are correlations for fluctuations in the tidal and supertidal frequency bands.

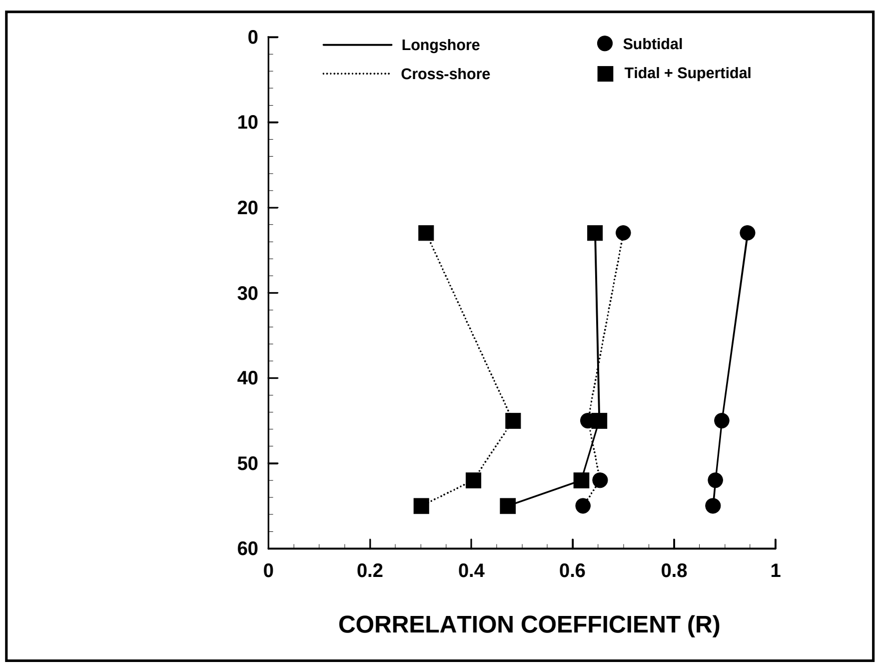

rents within 5 m of the bottom. Net offshore flows were weak and within the range of measurement and digitization errors in the current meter data (particularly for the film-recording meter). However, measurement errors were randomly distributed about zero for net cross-shore velocities (Figure 12). Net offshore flow was observed in 92 of 101 deployment-averaged near-bottom flows on the mainland shelf; it is likely that this was measurement and digitization errors.

Karl *et al*. (1980) measured near-bottom currents in 21 m and 60 m of water on the San Pedro Shelf (18-19 km upcoast from the primary mooring off Newport Beach) from mid-April to early June 1978 with tripod-mounted electromagnetic current meters. The net cross-shore component 1 m above the bottom was 2.3 cm/s offshore. This is comparable to the average net flow of 1.5 cm/s offshore for the combined spring data collected with SCCWRP current meters in 56 m of water off Newport Beach. Interestingly, net offshore flow was 2.3 cm/s during the spring deployment (4/17/90-5/25/90).

Figure 12.

Daily average longshore velocity and daily average cross-shore velocity of near-bottom currents on the mainland shelf off Southern California. Positive longshore velocities are upcoast flow and positive cross-shore velocities are onshore flow. Total number of data points is 2702 (83 month long deployments for about 7 meter-years) from all study sites.

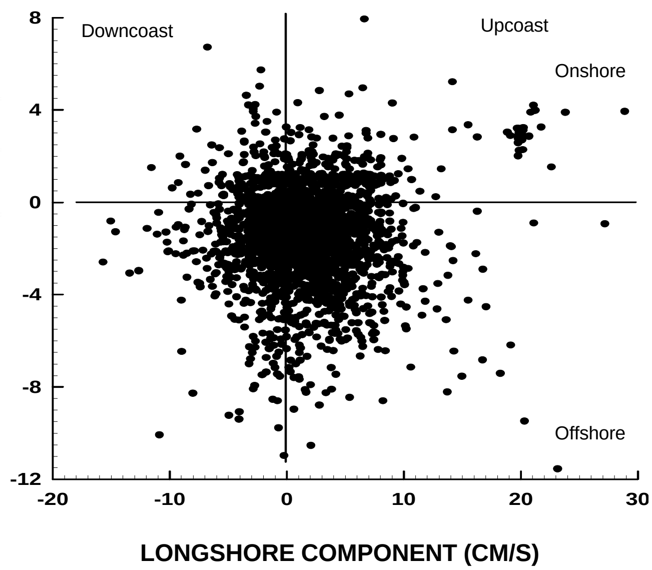

Differences Among Near-bottom Flows

Although near-bottom currents had a net offshore component in all areas on the mainland shelf, there were quantitative differences among areas. For example, net cross-shore flows off Palos Verdes were weaker than off Point Loma (Table 3). Offshore flows near the bottom varied with depth along the coast.

Karl *et al.* (1980) measured a net offshore flow of 0.4 cm/s in 21 m of water, which was about 15% of the net flow measured farther offshore in 60 m of water. We observed the opposite during 74 days in winter off Carlsbad: net near-bottom cross-shore speeds were 2.4 cm/s offshore in 25 m of water and 1.7 cm/s offshore in 45 m of water. During a 37-day summer deployment off Carlsbad, net cross-shore speeds were reduced, but were still offshore. Offshore net flow was 1.5 cm/s at the inshore mooring and 0.4 cm/s at the offshore mooring.

Off the East Coast, near-bottom offshore flows were measured on the outer shelf and upper slope in 80-1150 m (Wunch and Hendry 1972, Bumpus 1973, Beardsley *et al*. 1985, Butman 1988). The characteristics of these near-bottom flows differ from near-bottom currents off Southern California. Butman (1988) compared near-bottom (5-7 mab) and mid water (44-101 mab) currents at six moorings in 100-1150 m of water.

Near the bottom, net cross-shore flows were always offshore, but offshore speeds varied with water depth and peaked on the upper slope in 200-250 m of water. Off Southern California, there was no evidence for a net offshore flow on the upper slope (150-350 m) of water. Net off-shore near-bottom flows on the mainland shelf were confined to the lower 4-5 m of the water column and were absent or negligible 5-7 mab.

Importance of Near-bottom Currents for Particle Fates

Sediment traps at 0.5, 2, and 5 mab on the mainland shelf off Southern California collect a flux of material, including sediments, that decreases roughly exponentially with elevation above the bottom (Hendricks 1985, 1987, Hendricks and Eganhouse 1992). Recent studies of sediment resuspension on the shelf off Newport Beach frequently detected a nepheloid layer within 5 m of the bottom in 30-60 m of water. Near-bottom currents on the mainland shelf probably play an important role in the dispersal and fate of natural and effluent particles that settle to the bottom.

Correlations between near-bottom speeds and threshold speeds for sediment resuspension or deposition can result in a Reynolds flux of suspended solids that is not in the direction of net flow. Consider a hypothetical case where resuspension occurs when the net current and semidiurnal tidal current flow in the same direction (maximum bottom stress), and redeposition occurs when they flow in the opposite direction (minimum bottom stress). For clockwise rotation of the tidal vector, tidal flow has an offshore component for about 19% of the period, and an onshore component for 81% of the period; the net tidal-associated transport is 0.67 km onshore. Cross-shore transport associated with the net current is 0.25 km offshore. The resulting cross-shore transport between particle resuspenion and particle redeposition is 0.4 km onshore. For counter-clockwise rotation, tidal-associated transport is 0.67 km offshore, and transport associated with net flow is 0.25 km offshore; the resulting transport is 0.9 km offshore. In both cases, longshore transport is 0.35 km upcoast.

Net transport of resuspended particles depends on the relation between currents and conditions for sediment resuspension and redeposition. For some conditions, transport may be onshore even though net cross-shore flow is offshore. Although presently not well understood, conditions leading to sediment resuspension and redeposition are critical to estimating transport, dispersal, and fates of particles that settle to the bottom.

Near-bottom Ekman Flow

Several mechanisms have been proposed to explain near-bottom offshore flows (e.g., Buttman 1988; Garrett *et al.* 1993). Cross-shore flow may be associated with the formation of a bottom Ekman layer. The combination of friction with the bottom and the rotation of the earth results in a deflection of near-bottom flow to the left (for a person looking downstream). The presence of Ekman veering in bottom boundary layer currents has been observed on both coasts of the United States (Kundu 1976, Mercado and Van Leer 1976) and on the shelves of other continents (Dickey and Van Leer 1984).

Off Southern California, the net longshore flow of currents below the thermocline on the mainland shelf was generally upcoast. Therefore, on average, the effects of bottom friction may produce an offshore component to flow near the bottom. Conversely, during periods of downcoast flow there should be an onshore component to near-bottom flow. We tested whether Ekman flow produced the net offshore near-bottom flow by comparing the frequency of offshore flow during periods of upcoast flow with the frequency of offshore flow during periods of downcoast flow. If simple

Ekman flow was responsible for the net offshore current, offshore flow should have been more common during periods of upcoast flow.

The time scale to establish pressure gradients associated with Ekman flow is approximately the inertial period (22 h). The displacement of the daily-averaged observations in the low pass velocity time series to the right and down from two axes indicated a net tendency toward upcoast and offshore flows in near-bottom currents (Figure 12). About 65% of the daily average flows were upcoast and 29% downcoast; 6% had an average velocity <0.25 cm/s. Daily average cross-shore flows were offshore about 71% of the time and onshore about 18% of the time; 11% had an average velocity <0.25 cm/s. When the longshore flow was upcoast, the ratio of offshore to onshore flows was 4.7:1 (76% offshore, 16% onshore). When longshore flow was downcoast, the ratio was 3.3:1 (67% offshore, 20% onshore). Since we expect a ratio of 0.21 (=1/4.7) for a downcoast flow (based on the ratio for upcoast flow), simple bottom Ekman flow is probably not the primary driving force of the net offshore near-bottom current.

The question of the contribution of Ekman flow to the offshore motions is complicated by the density stratification of the water column, which is usually present off Southern California. In the presence of stratification, density gradients tended to suppress cross-shore flows after an initial set up interval. However, vertical mixing (across isopycnal surfaces) can still result in persistent cross-shore flows, with the direction of the flow changing with elevation above bottom (Garrett *et al.* 1993). There was not sufficient information for the mainland shelf to test this hypothesis.

Mixing and Current Fluctuations in Tidal and Supertidal Frequency Bands

Butman (1988) proposed a mechanism to generate a net near-bottom offshore flow that involves the interaction of cross-shore flows in the tidal and supertidal frequency bands, bottom friction, density instabilities, and vertical mixing. Off the northeastern United States, the strength of offshore flows in the subtidal (low-pass) frequency band are correlated with the strength of tidal and supertidal (high-pass) velocity fluctuations and an onshore Reynolds flux of density.

On the mainland shelf off Southern California, correlations were generally low (-0.20 to 0.10) between slow variations in the strength of short-period flows (tidal and supertidal frequency band) and slow changes (subtidal frequency band) in the strength of the offshore flow; correlations in a few deployments were substantially higher.

We examined the Reynolds density flux with measurements of currents and temperature at two moorings off Newport Beach between 1/25/92 and 2/25/92. Since the density of sea water on the mainland shelf off Southern California is inversely correlated with water temperature, we used the Reynolds temperature flux as a surrogate measure of the Reynolds density flux. The correlation between the Reynolds density flux and slowly varying changes in near-bottom flows was 0.42 for the primary mooring and 0.65 for the upcoast (3.1 km) mooring. The onshore density flux near the bottom (1-5 mab) almost disappeared 11 mab and remained near zero over the rest of the water column. The positive correlation in near-bottom waters indicated that an offshore flow was associated with an onshore density flux, which is in agreement with Butman (1988), but our correlations were weaker than his (0.75).

The Reynolds temperature flux was examined for temperature and velocity fluctuations in the subtidal frequency band. In near-bottom waters, there was a deployment-averaged offshore flux of density comparable in magnitude to the onshore Reynolds flux of density associated with fluctuations in the tidal and supertidal frequency bands. At time-scales of about a month, the near-bottom onshore Reynolds density flux associated with tidal and supertidal fluctuations was nearly canceled by the opposing flux associated with subtidal fluctuations. The relation between Reynolds fluxes of mass and net offshore flows in Southern California coastal waters was not clear.

Conclusions

Near-bottom currents on the mainland shelf off Southern California had several important characteristics that were not observed in mid water currents: 1) An offshore component was present in net (circa month long) near-bottom flows that was absent (or onshore) in mid water. The strength of the offshore component was comparable to the strength of the longshore component. 2) In near-bottom flows, fluctuations in semidiurnal tidal and supertidal frequency bands were enhanced, while fluctuations of subtidal frequency were reduced. Fluctuations associated with the first harmonic of the semidiurnal tide were occasionally present in near-bottom flows. 3) Bottom friction reduced the speeds of near-bottom currents to 75-80% of the speeds of mid water flows. Occasionally, near-bottom speeds exceeded mid water speeds. While the strength of the near-bottom currents varied with season, location, and water depth, they were limited to within about 5 m of the bottom.

Particles settling from the overlying water column are carried along by mid water currents that flow predominantly along the mainland shelf. Hence, settling particles tend to be deposited along isobaths. Near-bottom sediment trap and transmissometer studies suggested that these particles are resuspended many times. The thickness of the near-bottom nepheloid layer containing resuspended particles was nearly the same as the thickness of the near-bottom currents. Since near-bottom currents have a significant offshore component to net flow, they may be important in moving particles off the mainland shelf. However, more information is needed on the conditions leading to sediment resuspension and particle redeposition.

Near-bottom flows off the East Coast differ in several ways from near-bottom flows over the mainland shelf and upper slope off Southern California. Near-bottom currents off California were confined close to the bottom, and were not observed on the upper slope. The driving force for the near-bottom net offshore flows is unknown. The data were not consistent with the hypothesis that offshore flow was associated with simple Ekman flow. Butman (1988) proposed a mixing model that could generate an offshore near-bottom net flow. However, results from the mainland shelf off Southern California were consistent with some aspects of the hypothesis and inconsistent with others.

References

- Beardsley, R.C., D.C. Chapman, K.H. Brink, S.R. Ramp, and R. Schlitz. 1985. The Nantucket Shoals flux experiment. Part 1: A basic description of the current and temperature variability. *J. Phys. Oceanogr.* 15:713-748.
- Bumpus, D.F. 1973. A description of the circulation on the continental shelf of the United States. *Prog. Oceanogr.* 6:111-157.
- Butman, B. 1988. Downslope Eulerian mean flow associated with high-frequency current fluctuations observed on the outer continental shelf and upper slope along the northeastern United States continental margin: Implications for sediment transport. *Contin. Shelf Res.* 8:811-840.
- Dickey, T.D. and J.C. Van Leer 1984. Observations and simulation of a bottom Ekman layer on a continental shelf. *J. Geo. Phys. Res.* 89:1983-1988.
- Garrett, C., P. MacCready, and P. Rhines 1993. Boundary mixing and arrested Ekman layers: Rotating stratified flow near a sloping boundary. *Annu. Rev. Fluid Mech.* 25:291-323.
- Greene, C.S. and T.S. Sarason 1974. Cluster analysis of benthic communities. Pp. 23-31, *In:* Coastal Water Research Project 1974 Annual Report. Southern California Coastal Water Research Project, El Segundo.

- Greene, C.S. and R.W. Smith 1975. Numerical analysis of data on a benthic community. Pp. 69-77, *In:* Coastal Water Research Project 1975 Annual Report. Southern California Coastal Water Research Project, El Segundo.
- Hendricks, T.J. 1983. Numerical model of sediment quality near an ocean outfall. Rep. to NOAA ERL/ PMEL. Southern California Coastal Water Research Project, Long Beach. 275 pp.
- Hendricks, T.J. 1987. A study of sediment composition, transport, and deposition off Palos Verdes. Final Rep. to County Sanitation Districts of Los Angeles County, Whittier. Southern California Coastal Water Research Project, Long Beach. 46 pp.
- Hendricks, T.J. 1990. Analysis of cross-shore transport off Point Loma. Rep. to Eng. Sci. Inc., La Jolla. Southern California Coastal Water Research Project, Long Beach. 71 pp.
- Hendricks, T.J. 1992. Orange County currents, Phase II - SCCWRP measurements. Rep. to Co. San. Dist. Orange Co. Southern California Coastal Water Research Project, Long Beach. 170 pp.
- Hendricks, T.J. and R. Eganhouse 1992. Modification and verification of sediment deposition models. Rep. to Calif. State Water Res. Ctrl. Brd., Southern California Coastal Water Research Project, Long Beach. 330 pp.
- Karl, H.A., D.A. Cacchione, and D.E. Drake. 1980. Erosion and transport of sediments and pollutants in the benthic boundary layer on the San Pedro Shelf, Southern California. U.S. Dept. Int., USGS, Open-File Rep. 80-386. 101 pp.
- Kundu P.K. 1976. Ekman veering observed near the ocean bottom. *J. Phys. Oceanogr*. 6:238-242.
- Mercado, A. and J. Van Leer. 1976. Near-bottom velocity and temperature profiles observed by Cyclesonde. *Geophys. Res. Lett*. 3:633-636.
- Ontnes, R.K. and L. Enochson. 1978. Applied time series analysis. Volume I: Basic techniques. John Wiley and Sons, NY.
- Press, W.H., S.A. Teukolsky, W.T. Vetterling, and B.P. Flannery. 1992. Numerical recipes in FORTRAN, Second Ed., Cambridge Univ. Press, NY.
- SCCWRP see *Southern California Coastal Water Research Project.*
- Southern California Coastal Water Research Project. 1986. Sedimentation, resuspension, and transport of particulates. Pp. 26-29, *In*: Coastal Water Research Project Annual Rep. 1976. Southern California Coastal Water Research Project, Long Beach.
- Wunch, C. and R. Hendry. 1972. Array measurements of the bottom boundary layer and the internal wave field on the continental slope. *Geo. Fluid Dynm*. 4:101-145.

Acknowledgements

Author Terry Hendricks thanks H. Stubbs, D. Diehl, M. Moore, and P. Hershelman for organizing cruise activities, maintaining current meters and moorings, and conducting the “at sea” operations. He thanks the County Sanitation Districts of Los Angeles County, County Sanitation Districts of Orange County, the City of Los Angeles, and the City of San Diego for their vessels and crews who deployed, recovered, and serviced the moorings. He appreciates the assistance of Hydraulics Laboratory personnel at Scripps Institution of Oceanography for their assistance in the calibration of the current meters.